The EuroBiotech Journal
RESEARCH ARTICLE
Biomaterials

Probiotic-infused Mixed Polymeric Nanoparticles Co-incubated with Antibiotics: An Alternative Approach to Combat Drug-resistant Bacteria

Anbazhagan Thirumalai[1], Sampreeti Chatterjee[1], Pemula Gowtham[1], Koyeli Girigoswami[2], Agnishwar Girigoswami[1*]

Abstract

The frequent rise of antibiotic-resistant bacteria is due to the increasing use of antibiotics in the healthcare system. Probiotics could offer a potential alternative, although their efficacy tends to be diminished in the presence of antibiotics, rendering co-fortification an impractical solution. Stand-alone probiotics cannot completely counteract the effects of antibiotics and often die off in the stomach due to the lower acidic pH. Similarly, antibiotics significantly reduce the action of probiotics; as a result, their therapeutic potential is diminished. Based on the biofilm protection characteristic, chitosan and alginate nanogel are used to encapsulate probiotics with temporary protection against antibiotics, enabling the simultaneous delivery of probiotics and antibiotics. This study involved encapsulation of the probiotic within chitosan-coated alginate nanoparticles (Cs-Alg+ProB NPs), which were made using the ionic gelation technique. The physicochemical characteristics, probiotic release profile across varying pH levels, swelling properties, coincubation of probiotics with antibiotics, and in vitro toxicity evaluation of the produced nanocomplex were examined. The hydrodynamic size of nanoparticles increased from 295.3±7.13 nm to 328.7±13.07 nm after probiotic encapsulation, confirming successful loading, as supported by zeta potential changes. Enhanced probiotic release and swelling were observed under acidic pH. The Korsmeyer-Peppas model indicated Fickian diffusion as the release mechanism. Coincubation with amoxicillin demonstrated that encapsulation protects probiotics, a finding that can be extended to provide therapeutic benefits against MDR bacteria to protect public health.

Keywords: Health care; polymer nanoparticles; encapsulation; well-being; antibiotic resistance.

Introduction

Due to the selective pressure that prolonged and extensive use of antibiotics has placed on microbial populations, bacteria and fungi have developed resistance mechanisms against multiple drugs, a phenomenon known as multidrug resistance (MDR) (1, 2). Owing in large part to the extensive and frequently uncontrolled use of antibiotics in human medicine, veterinary care, aquaculture, and agriculture, antibiotic resistance has emerged as a serious global health concern (3, 4). Antimicrobial-resistant bacteria have emerged and spread more quickly as a result, making common infections harder to treat. Public health is seriously threatened by this growing problem since the reduced effectiveness of antibiotics makes it more difficult to control infections, which raises the risk of serious or fatal consequences, increases morbidity, and speeds up transmission (5, 6). Bacterial resistance to currently available treatment strategies has made it difficult to treat against pathogens, including *Pseudomonas aeruginosa* and multidrug-resistant *Enterobacteriaceae*, as most of the antibiotics are no longer effective. The WHO has listed antibiotic resistance as one of the top 10 global public health threats, underscoring its severe challenges to public health. As this crisis continues to escalate, the importance of novel approaches to combat resistance and preserve established antimicrobial treatments is heightened (7, 8). To contain another wave of resistance, these spreading epidemics underscore the urgent necessity to use antibiotics wisely and invest in alternative approaches to treatment as well as scientific discovery to understand and overcome them (9, 10). Antibiotic resistance has been labelled as "the silent tsunami of modern medicine" (11). Resistance is a result of

[1]Medical Bionanotechnology, Faculty of Allied Health Sciences FAHS), Chettinad Hospital & Research Institute (CHRI), Chettinad Academy of Research and Education (CARE), Kelambakkam, Chennai, TN-603103, India.
[2]Medical Bionanotechnology Lab, Department of Obstetrics and Gynaecology, Saveetha Medical College, Saveetha Institute of Medical and Technical Sciences, Thandalam, Chennai, 602105, India

***Corresponding author:**
Agnishwar Girigoswami
Email: agnishwarg@gmail.com
ORCIR iD: 0000-0003-0475-2544

DOI: 10.2478/ebtj-2026-0007

selection. In a population of parasites, there can be genetic heterogeneity, including mutations that are beneficial to the microbe's survival under antimicrobial exposure. Resistance to the antibiotics may be the organism's intrinsic functional ability (12). Vancomycin is largely ineffective against Gram-negative bacteria because it cannot penetrate the outer membrane. *Klebsiella sp*. has an intrinsic resistance to ampicillin due to beta-lactamase synthesis. *Pseudomonas aeruginosa* is inherently insensitive to tetracycline, trimethoprim, sulphonamides, and chloramphenicol. Resistance can also develop extrinsically via the development of mutations. These mutations occur as a survival mechanism in response to antibiotics. The widespread use of antibiotics results in an increase in resistant strains, contributing to antimicrobial resistance (13).

Mutations occurring at the chromosomal level may lead to greater expression of antibiotic-inactivating enzymes (14). Resistance genes can be transferred from one bacterial species/genus to another via horizontal gene transfer techniques such as transformation, transduction, and conjugation. Mobile genetic elements carrying one or more resistance factors can include plasmids, like the well-known resistance plasmid 1 or R1 plasmid found in Gram-negative bacteria (GNB), along with transposons (for example, Tn5053) and integrons (such as the Verona integron-encoded metallo-beta-lactamase identified in GNB) (15, 16). In the case of GNB, particularly within the Enterobacteriaceae family, evidence indicates that resistance genes, along with associated insertion sequences, are frequently clustered within extensive multiresistance regions (MRRs) on plasmids (17). The Centers for Disease Control and Prevention (CDC) stated that annually, more than 2 million individuals in the USA suffer from infections caused by antimicrobial-resistant pathogens, leading to over 23,000 fatalities (18). Globally, around 700,000 deaths each year are attributed to antimicrobial resistance, and projections suggest this number could rise to 10 million annually by 2050 (19-21).

Probiotics have been introduced as an effective solution to this problem. It has been successfully used for treating fatal infections and also used in situations where antibiotics have been rendered useless (22). Probiotics are essentially live, weakened microbes that provide health benefits if administered in appropriate quantities. They have come up with an impactful solution to the problem of antibiotic-resistant bacteria (ABR). Certain probiotics can inhibit pathogenic microorganisms by producing antimicrobial compounds and organic acids (23, 24). The co-administration of probiotics with conventionally used antibiotics has shown potential against ABR and other complex infections. Probiotics are essentially bacteria; they are very vulnerable to antibiotics and cannot coexist when administered together (25). Transformation of probiotic strains using recombinant plasmids carrying antibiotic-resistant genes is a common but inefficient approach that leads to the development of permanently resistant strains. This may cause threats of pathogenicity and proclivity to transfer resistance genes to other bacteria (26, 27).

An alternative strategy to overcome this issue is the encapsulation or covering of probiotics to enhance their therapeutic efficacy in the presence of antibiotics. This encapsulation protects probiotics against antibiotics without the need for genetically modified organisms (28). While several encapsulation technologies have been developed to enhance probiotic survival, there are still key limitations that remain unresolved. Conventional encapsulation approaches often provide only partial protection in the harsh gastrointestinal environment, resulting in low viability of probiotics at the site of infection. While certain antibiotic-resistant infections may survive after treatment using a conventional antibiotic, we predict that the co-administration of encapsulated probiotics and conventional antibiotics has the potential to control drug-resistant pathogens and also enhance therapeutic efficacy. Encapsulation of probiotics secures their vitality along with easing the delivery mechanism to the target location (29). Vega-Carranza et al. *Bacillus licheniformis* entrapped in an alginate microparticle by the ionic gelation method, which resulted in a significant increment in bacterial stability (30). Their findings demonstrated that this encapsulation method enhanced not only probiotic survival under stressful conditions but also a more targeted release in the mock shrimp gastrointestinal tract. The encapsulated probiotics exhibited high encapsulation efficiency (~99.9%) and maintained better stability during storage compared to free bacteria. Importantly, survival studies revealed that alginate microparticles provided a protective effect, allowing approximately 51% of viable probiotics to reach the shrimp intestine, in contrast to only 27% viability observed with free bacteria (30). Yuan *et al*. demonstrated that alginate hydrogel-encapsulated *Bifidobacterium breve* exhibited superior protection against simulated gastric fluid and tetracycline exposure, conditions under which unencapsulated bacteria failed to survive (31). Notably, this encapsulation strategy not only preserved probiotic viability but also enabled a synergistic effect with tetracycline, leading to the eradication of tetracycline-resistant *Escherichia coli* adhering to intestinal epithelial layers while maintaining epithelial barrier integrity. In comparison, other nanomaterial-based shells, such as SiO_2 yolk–shells or ZIF-8 mineralization, offered less protection or caused detrimental effects on bacterial cell walls. These findings highlight the potential of nanomaterial-based encapsulation, particularly alginate hydrogels, in safeguarding probiotics through gastrointestinal transit and enhancing their functional efficacy in combating pathogenic infections (31).

Our encapsulation strategy is based on alginate and chitosan because biopolymers are a better choice for developing nano-delivery systems to obtain biodegradability, biocompatibility, hydrophilic, and protective nature (32, 33). Polyionic hydrogel formation from biodegradable cationic and anionic biopolymers is the most favorable method for drug entrapment, drug solubility, and drug delivery in a controlled manner (34, 35). Two natural biopolymers, chitosan and alginate, have received huge attention in the pharmaceutical industries for the nanoformulation of life-saving drugs to increase the drug's half-life and bioavailability and protect the drug from enzymatic degradation. Mixed polymer nanogels have proved to sol-

ubilize both hydrophilic and hydrophobic drugs readily (36). Alginates are nonimmunogenic, non-toxic, biodegradable, mucoadhesive, hemocompatible polymers that form hydrogels under mild conditions, ensuring high probiotic viability during encapsulation (37). Alginate is mostly used in wound dressing, tissue, and bone engineering, artificial scaffolding for the fabrication of cells and tissues, and cellular drug delivery (38). However, alginate beads alone can be porous and susceptible to premature release or degradation in acidic gastric environments. Coating with chitosan enhances the structural integrity of the hydrogel, reduces porosity, and provides an additional protective barrier against harsh gastrointestinal conditions. Chitosan's polycationic nature promotes strong electrostatic interactions with negatively charged alginate, improving mechanical stability and modulating the release profile. Chitosan has its own bioactive properties that promote the adhesion and colonization of probiotics on the intestinal mucosa (39). Chitosan has been used to coat alginate in order to enhance the shelf life, half-life in the circulation, and bioavailability due to the positive charge on the surface of nanoparticles (40, 41). The alginate-chitosan system utilizes the high encapsulation efficiency and biocompatibility of alginate, and the protective, mucoadhesive, and stabilizing properties of chitosan, leading to better probiotic delivery and therapeutic efficacy than either polymer alone (32).

The present study is directly aimed at filling this gap and is using as well as developing a protective carrier system–Chitosan-alginate nanoparticles. What was new about our method was the use of alginate and the complementary properties of alginate with chitosan. Not only does this dual-polymer nanocarrier bolster probiotic survival during gastric transit and colonization upon reaching the infection site, but it also serves as an alternative therapeutic mechanism against the resistant bacteria. This method enables the simultaneous oral administration of probiotics and antibiotics (amoxicillin) to achieve a higher therapeutic outcome. Amoxicillin was chosen for this study because it is the most widely prescribed broad-spectrum β-lactam antibiotic, used for gastrointestinal and respiratory infections. Furthermore, the widespread use of this antibiotic in humans has resulted in the emergence of resistant bacterial strains, making it a clinically relevant model drug for the study of probiotic-antibiotic interactions. Further research has also been implemented to provide evidence of physical interactions of antibiotics and gut microbiota, and examples such as amoxicillin, which severely disrupt gut microbiota, emphasize the need to develop approaches like co-delivering probiotics to alleviate the side effects of antibiotics. In light of the importance of this advancement and the available emerging nano-enabled delivery systems, we evaluated the potential of the composite chitosan-alginate nanoparticles (Cs-Alg NPs) for probiotic encapsulation.

2. Materials and methods

2.1. Materials

Sodium alginate (molecular weight ≈200-400 kDa), chitosan (molecular weight ≈150-300 kDa), Lactobacillus De Man, Rogosa, and Sharpe (MRS) broth, Lactobacillus MRS agar, Luria broth (LB), Muller Hinton Agar (MHA), Alamar blue, and amoxicillin were obtained from Himedia. Calcium chloride, sodium hydroxide (NaOH), and acetic acid were purchased from Rankem, India. Probiotics (containing *Lactobacillus acidophilus*, *Lactobacillus plantarum*, *Lactobacillus casei*, and *Lactobacillus rhamnosus*) were commercially purchased from Eris Life Science Pvt Ltd., India.

2.2. Synthesis of probiotic-loaded mixed polymer nanoparticles

Chitosan-alginate nanoparticles (Cs-Alg NPs) were synthesized using a standard protocol with modifications (33). At first, 6 mM sodium alginate (Alg) was dissolved in 10 mL of distilled water, and its pH was adjusted to 5.5. Then 0.01g/mL of chitosan (Cs) was dissolved in 10 mL of 0.1% acetic acid, and its pH was adjusted to 5.4 using sodium hydroxide. A 30mM calcium chloride solution was made, and a probiotic capsule was added and dissolved in it. Probiotic-loaded chitosan-alginate nanoparticles (Cs-Alg+ProB NPs) were prepared by a two-step method. 2 mL solution of calcium chloride containing the probiotic was added dropwise to the Alg solution and stirred for 10 mins. The chitosan solution was then added to the aforementioned mixture after stirring, and stirred for another hour. Post stirring, the resultant opalescent solution is left undisturbed to incubate overnight to form uniform-sized NPs. The obtained monodispersed solution was centrifuged at 3500 rpm for 25 mins, and the pellet was collected and resuspended in distilled water. This procedure is repeated thrice to ensure complete removal of unreacted reagents. Finally, the purified pellet (Cs-Alg+ProB NPs) was dissolved in 10 mL of 7.4 pH PBS and stored for further assessment.

2.3. Characterization

We used a Bruker-Alpha FTIR/ATR spectrometer to look for functional groups in the Cs-Alg NPs we made. A scanning electron microscope (SEM) model number FEI Quanta 200-FEG was used to look at the surface properties of the NPs. We used a Malvern Nano ZS90 particle size analyzer (Worcestershire, UK) to measure the particles' hydrodynamic size (dH) and surface zeta potential. This analyzer works by using dynamic light scattering.

2.4. Encapsulation efficiency and Release kinetics

We used a spectrophotometer to measure the absorbance at 600 nm to find out how well the probiotics were encapsulated in Cs-Alg NPs in terms of encapsulation efficiency. We used a standard protocol to study how quickly probiotics were released from the synthesized Cs-Alg+ProB NPs in phosphate-buffered solution (PBS) and HCl/KCl buffer to establish the release profile (42). The Cs-Alg+ProB NPs were loaded into activated dialysis bags and suspended in 25 mL of buffers at room temperature under constant stirring conditions. After immersion, 2 mL of the buffer was collected at regular intervals till 600 mins, and

2 mL of fresh buffer was replaced immediately. The amount of probiotics released from the Cs-Alg NPs was measured using the spectrophotometric analysis (OD at 600 nm), and CFU/mL of probiotic growth was done in an MRS agar plate.

Korsmeyer-Peppas (KP) model or the "power law" is employed to explain the driving force of molecular transport from Cs-Alg+ProB nanoparticles. The potential use of this semi-empirical model can be foreseen in cases where the release rate profile does not correspond to some easily interpretable mechanism or when the combined occurrence of several diffusion and polymer relaxation phenomena is suspected (33, 43). It represents the net effects of multiple kinetic processes: penetration of water molecules into the polymeric network; swelling, relaxation, and rigidification (loss of potential to deform plastically) by the solid matrix; and finally, erosion or structural breakdown. Incorporating the simultaneous mechanisms, the KP model offers a comprehensive basis to analyze complex profiles of release experienced by systems. The probiotic release profile from Cs-Alg nanoparticles was also determined using this model by the following equation [1].

$$\frac{Q_t}{Q_\infty} = kt^n \quad [1]$$

where Q_t is the number of molecules released from the encapsulation at time t. Whereas Q∞ represents the sum of molecules released over an infinite or indefinite amount of time. The constant *k* reflects the structural and geometric attributes of the nanoparticle-based delivery system, while the release exponent *n* provides insight into the underlying mechanism governing probiotic release from the synthesized polymeric nanoparticles. Together, these parameters help characterize how the matrix architecture influences the overall release behavior.

2.5. Swelling tests

The swelling properties of the nanoparticles were evaluated according to the method reported by Girigoswami et al. (36). This test not only helps shed some light on how well the nanoparticles interact in water, but through swelling, it can also assess, to a degree , how much water absorption the particles are capable of. These swelling behaviors are related to the drug release behaviors; generally, drugs will be released more rapidly with a higher swelling ratio and more slowly with a lower swelling ratio. Equilibrium mass swelling (EMS) was measured at various time intervals to estimate the degree of water uptake. To do so, the dry Cs–Alg particles were immersed in two kinds of medium: a hydrochloric acid/potassium chloride (HCl/KCl) buffer set at pH 2.2 to mimic gastric conditions and a PBS solution at pH 7.4 to simulate body conditions, bedroom environment, and a 95 °C control (both room temperature). The nanoparticles were occasionally withdrawn from the medium, gently blotted with absorbent paper to eliminate surface water, and weighed. Upon weighing, they were transferred back to the swelling medium and reincubated for subsequent determinations.

$$\%EMS = \frac{M_s - M_d}{M_d} \times 100 \quad [2]$$

Where %EMS is the swelling index, M_s and M_d are the mass of the swollen NPs and the dried NPs at 45 °C, respectively.

2.6. MIC of amoxicillin

To evaluate the minimal inhibitory concentration (MIC) of amoxicillin, probiotics were used.

Mueller-Hinton agar plates were prepared, and the inoculum (100µL) of probiotic strains was spread on the agar surface. Then 6 wells were made into the agar, and 50 µL of different concentrations of amoxicillin was added (0µM, 10µM, 20µM, 40µM, and 50µM). Then the plates were then incubated overnight at 37 °C. MIC was calculated by measuring the formed inhibitory zone surrounding wells against the microbes.

2.7. Coincubation of probiotics with antibiotics

In MRS broth medium, free probiotics and NPs loaded probiotics were incubated with and without amoxicillin in a test tube at 37 °C for 24 h. From this coincubated medium, 100 µL was taken and inoculated in MRS agar and incubated for 12 h at 37 °C. The plating and counting of the probiotics' growth were analyzed using the colony counting method and by measuring optical density (OD) at 600 nm.

2.8. AlamarBlue assay

AlamarBlue dye 100 µg/mL was added to 2 mL of samples (both free and NPs loaded probiotics) and then incubated at 37 °C for 3h. The fluorescence signal was recorded every 1h with a spectrofluorometer at 530 nm as excitation and 560 nm as emission.

2.9. Coincubation of probiotics with antibiotics

Staphylococcus aureus (OD 2.4) was grown in Luria broth, from which 10 mL was collected, centrifuged at 5000 rpm, and resuspended in PBS. For co-incubation, 1 mL of free and encapsulated probiotics was added to 10 mL of Luria broth, followed by the addition of 500 µL of *S. aureus* in the test tube. The tubes were sealed and incubated for 24 h at 37 °C. The growth of probiotics and pathogens was assessed through the catalase assay.

2.10. *In vitro* cell viability assay

The toxicity of synthesized Cs-Alg NPs was assessed by conducting an MTT assay based on the procedure described by Girigoswami *et al.* (44). Briefly, normal fibroblast (V79) cells were maintained in complete DMEM and allowed to grow for 24 hours at 37 °C in a humidified incubator set to 5% CO_2. Approximately 2.7×10^5 cells/well were seeded in 48-well plates and allowed to incubate for an additional 24 h. The cells were exposed to Cs-Alg NPs at varying concentrations of 10 to 100 µg/mL and incubated for another 24 h. After incubation, 50 µL

of MTT solution (5 mg/mL) was added to each well in the dark without light degradation. Following treatment, the plates were incubated for 4 h to permit living cells to reduce MTT into formazan crystals. Dimethyl sulfoxide (DMSO) was added to the resulting formazan, and 570 nm absorbance was measured by a microplate reader after incubation. Cell viability (%) was calculated as follows [3]

$$Cell\ viablity\ (\%) = \frac{OD\ of\ sample}{OD\ of\ control} \times 100 \qquad [3]$$

2.11. Statistical analysis

The graphical representation of the obtained values is shown as the mean ± SEM, based on three sets of experimental data. One-way ANOVA was used to determine the significance ($p < 0.05$), and Microcal Origin was applied for the analysis.

3. Results and discussion

The copolymer and polycationic material nanocomposites have demonstrated potency as a drug carrier. An alginate core was produced in this work using the ionotropic gelation method. Alginate consists of sequences of monosaccharide residues, including both mannuronic and guluronic acid moieties, capable of ionic crosslinking with divalent cations. In a single film, calcium (Ca^{2+}) was incorporated as a divalent cation for the formation of a crosslinked hydrogel. Subsequently, the surfaces were coated with a polycation chitosan to produce stable probiotic delivery units. Due to unique physicochemical and biological properties, including hydrophilicity, high water holding capacity comparable to that of native soft tissues, obvious bioresponses, and versatile structure, among others, alginate and chitosan have gained much attention as promising candidates for therapeutic purposes in tissue regenerative medicine as well as wound healing. Both polymers exhibit excellent biocompatibility and biodegradability, making them well-suited for biomedical use. The incorporation of alginate into chitosan matrices significantly enhances the mechanical integrity of the composite system. Furthermore, as a polyanionic polymer, alginate can form polyelectrolyte complexes with the cationic chitosan via electrostatic interactions between the carboxyl groups of alginate and the amino groups of chitosan,

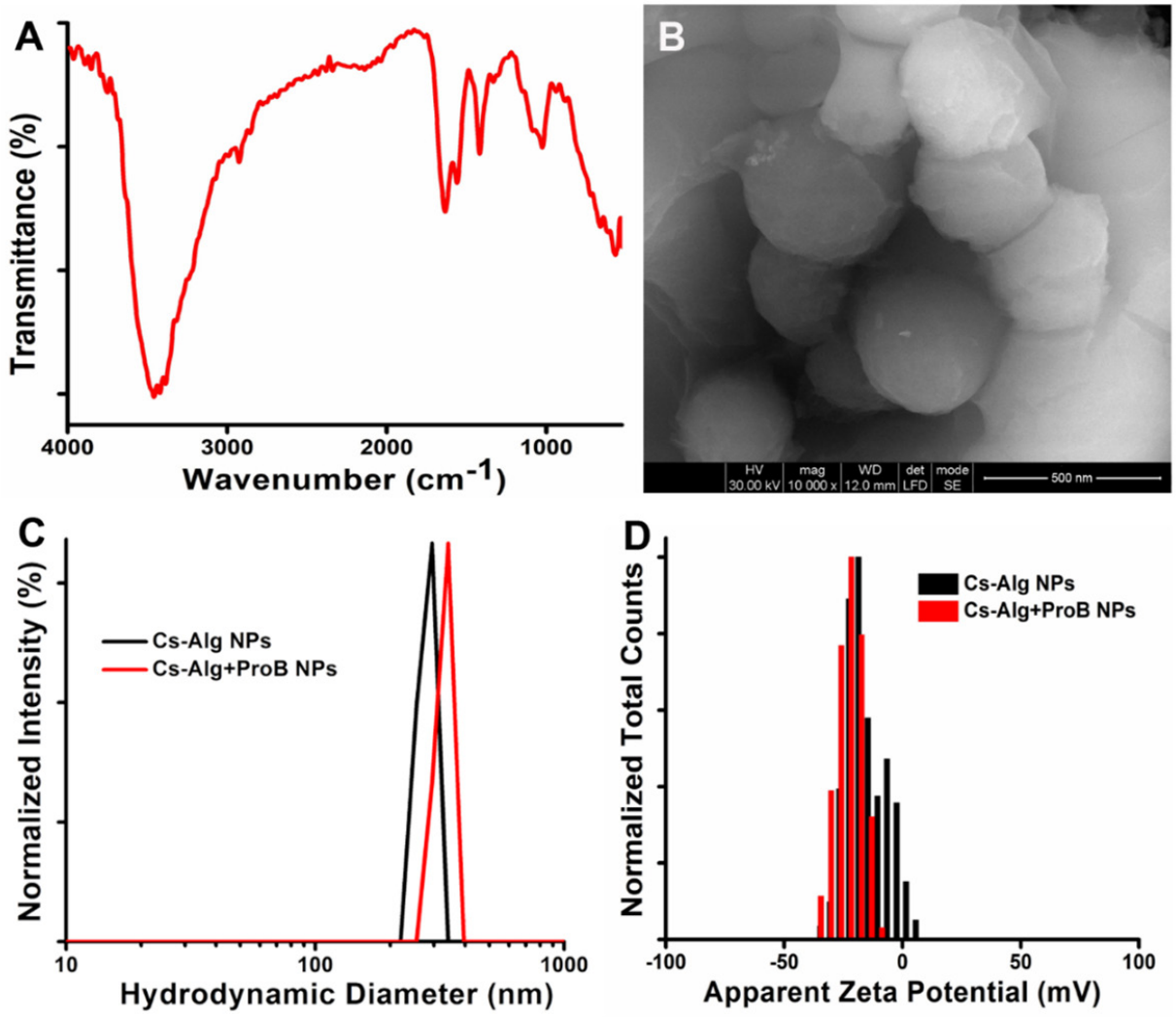

Figure 1. (A) FTIR spectra of Cs-Alg NPs. **(B)** SEM image of Cs-Alg NPs. **(C)** Hydrodynamic diameter of Cs-Alg NPs and Cs-Alg+ProB NPs. **(D)** Zeta potentials of Cs-Alg NPs and Cs-Alg+ProB NPs.

thereby improving the material's physicochemical stability and functional performance in biological environments.

3.1. Physicochemical characterization

The surface functional groups and chemical composition found in the synthesized Cs-Alg NPs are shown in **Figure 1A**. The FTIR spectra were obtained over the range of 500 to 4000 cm^{-1} using KBr as a standard. The band at 671 and 580 cm^{-1} corresponds to the C-Cl stretching vibrations of alkyl groups. The distinct band at 1022 cm^{-1} signifies C-O-C stretching, suggesting the presence of saccharide moieties within the alginate structure. Furthermore, the bands at 1423 and 1614 cm^{-1} are assigned to symmetric and asymmetric stretching of carboxylate groups, respectively. The amine-II bands of chitosan appear at 1554 cm^{-1} in the Cs-Alg complex, while the stretching vibrations of -OH & $-NH_2$ are observed at 3451 cm^{-1}, indicating the successful formation of blended polymer NPs. The presence of all these characteristic IR bands confirms the effective synthesis of Cs-Alg nanoparticles.

The surface morphology of the Cs-Alg NPs was determined by SEM images. **Figure 1B** illustrates the formation of Cs-Alg nanoparticles, which appear uniformly distributed and exhibit a spherical morphology. The average particle size of the Cs-Alg NPs was determined to be 287 nm ± 09 nm. By using the particle size analyzer, the colloidal properties in terms of hydrodynamic diameters and zeta potential of the chitosan-alginate NPs and probiotics-loaded chitosan-alginate NPs were identified based on the major scattering peak. **Figure 1C** shows that the average hydrodynamic diameter (dH) of the Cs-Alg NPs was recorded at 295.3±7.13 nm, whereas the Cs-Alg+ProB NPs exhibited a dH of 328.7±13.07 nm. The polydispersity index (PDI), a unitless measure, was employed to assess the distribution of particle sizes. The PDI derived from the autocorrelation function varied between 0.01 and 0.7 for defining monodispersed distribution in colloidal nanoparticle solutions (45). The PDI was found to be 0.384 for the Cs-Alg NPs and 0.329 for the Cs-Alg+ProB NPs. This PDI value suggests that both the synthesized Cs-Alg NPs and the probiotics-loaded Cs-Alg NPs are monodisperse and relatively uniform as per the above range. The zeta potential of the Cs-Alg NPs was measured at -18.3 mV, indicating a stable colloidal system. In contrast, the Cs-Alg+ProB NPs displayed a slightly lower negative zeta potential of -22 mV (**Figure 1D**). Measuring zeta potential is essential for understanding NPs stability, as their surface charge influences their colloidal properties. The variations in dH and surface charge values between the blended polymer NPs and probiotics-loaded NPs can be attributed to changes in their microenvironment, confirming the successful encapsulation of probiotics within the Cs-Alg NPs.

3.2. Release kinetics

The encapsulation efficiency (EE) of Cs-Alg+ProB NPs was calculated spectrophotometrically by recording the OD of the probiotics at 600 nm, and it was found to be 97.3 %. *In vitro* probiotics release rate was calculated via the spectrophotometric and colony count (CFU/mL) method. The cumulative release of probiotics from the synthesized blended polymer NPs in two release media for 600 mins is shown in **Figure 2A**. It was noted that the release of probiotics amounted to 65% at 2.2 pH and 47% at 7.4 pH from the Cs-Alg NPs, indicating a superior release in acidic environments, which resembles the gastric environment. An initial burst release was observed within the first 100 minutes, likely attributed to weakly bound probiotic cells on the exterior surface of the nanocarriers. The increased release at low pH arises from protonation, which induces weakening of the electrostatic interaction between chitosan and alginate. Acidic conditions cause polymer swelling and partial destabilization of the Cs-Alg matrix, leading to rapid release of surface-bound probiotics, followed by a controlled and sustained release phase over an extended period (46, 47). Notably, the increased probiotic release under acidic conditions suggests the system's suitability for oral delivery targeting the gastric environment, making it a promising approach for stomach- and gastric-related therapeutic applications.

The data collected from the release kinetics study was further examined using the KP model to determine the exact release mechanism working in the formulated nanoparticles. This model helps to understand whether the drug release procedure is governed by diffusion, erosion, or a combination of both. The following plots, shown in **Figures 2B and 2C,** depict $Qt/Q\infty$ plotted against time. The correlation coefficient (r), release rate constant (k), and release exponent (n) parameters calculated from the KP model for two different pH mediums of probiotics in Cs-Alg NPs are shown in **Table 1**. At $n \leq 0.45$, the release follows the mechanism of case I transport (Fickian diffusion). Alternatively, when n is equal to or greater than 0.89, the release profiles follow Case II transport, i.e., relaxation of the polymer network after swelling, referred to as anomalous diffusion and non-Fickian diffusion, respectively. An n in the range from 0.45 to 0.89 means an irregular or anomalous transport. These results proposed that the release control type could be a combined form of Fickian diffusion and polymer matrix erosion. More precisely, the release exponent for probiotics from Cs-Alg NPs was 0.240 at pH 2.2 and 0.353 at pH 7.4.

Table 1. The r, k, and n were assessed with the KP model to describe how probiotics are released from Cs-Alg NPs in various release conditions.

Release medium	pH 2.2	pH 7.4
r	0.930	0.922
k	11.085	8.340
n	0.240	0.353

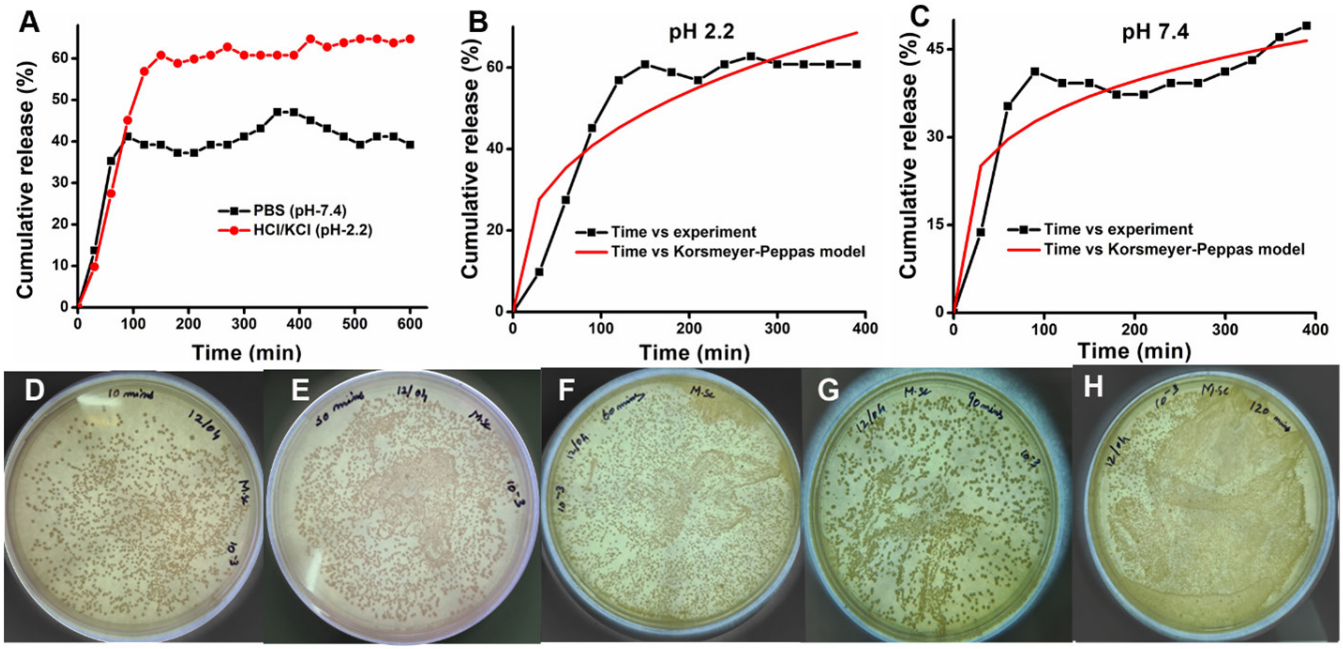

Figure 2. **(A)** Cumulative release profile of probiotics from Cs-Alg NPs in different media. KP model to fit the release profile of probiotics from Cs-Alg NPs in pH 2.2 **(B)** and pH 7.4 **(C).** Released probiotics from Cs-Alg NPs after 10 mins **(D),** 30 mins **(E)**, 60 mins **(F)**, 90 mins **(G)**, and 120 mins **(H)** to find their CFU/mL.

As both values are less than 0.45, the release behavior is indicative of Fickian diffusion, and the release rate of probiotics was mainly limited by the diffusion of probiotics through the polymer rather than polymer relaxation or degradation, leading to a relatively slow and sustained release manner. Probiotic release rate was also monitored via colony count (CFU/mL) as shown in **Figure 2 D, E, F, G, and H**. Dialysis solution of the probiotics released from the NPs was collected at regular intervals (10, 30, 60, 90, and 120 mins). The collected samples were diluted and evenly distributed over prepared MRS agar media plates, then incubated at 37°C for a duration of 12 h. Post incubation, colonies were counted, and CFU/mL was recorded as 1.2×10^5, 2.0×10^5, 3.7×10^5, 4.8×10^5, and 5.6×10^5, respectively. Thus, it can be concluded that the probiotic was released in a constant flow from the NPs.

3.3. Swelling assay

The swelling assays of Cs-Alg NPs were carried out in PBS and HCl/KCl medium at ambient temperature. The equilibrium mass swelling of Cs-Alg NPs was determined following a 10 h incubation period using Equation [2]. Initially, the mass swelling at pH 7.4 increased over time, but eventually, it plateaued **(Figure 3A)**. The hydration of hydrophilic groups in alginate and chitosan primarily drives the swelling behavior of the Cs-Alg complexes. There has been the penetration of free water into the Cs-Alg, which has filled the voids within the polymer-

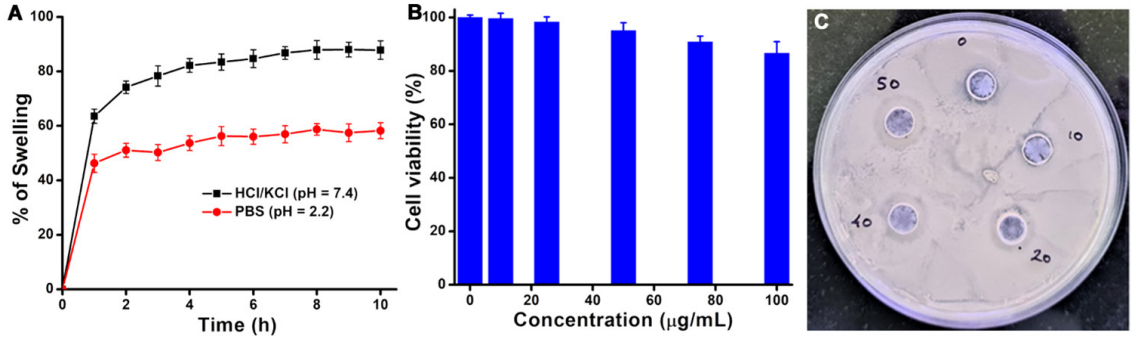

Figure 3. **(A)** Percentage swelling of Cs-Alg NPs in PBS and HCl/KCl buffer. **(B)** MTT assay for assessing cell viability in V79 fibroblast cells. **(C)** Antibiotic sensitivity to find MIC using the well-diffusion method.

ic matrix, leading to the observed swelling. When substantial interaction takes place between two polymer chains within the blended polymer NPs, the extent of swelling diminishes accordingly. The maximum swelling was observed at pH 2.2 due to the increased protonation of the -NH_2 groups found in chitosan, transforming them into ammonium ions. The osmotic pressure decreases at lower pH because the repulsive forces from the charged ammonium ions increase, thereby promoting the swelling behavior of Cs-Alg NPs.

3.4. Toxicity assessment

The biocompatibility of Cs-Alg NPs as a potential nanocarrier was assessed using the MTT assay to measure cellular viability in V79 cell lines (**Figure 3B**). The mixed polymer NPs demonstrated negligible toxicity (more than 85% of cells are viable) following 24 h of incubation at various concentrations from 10-100 µg/mL under physiological conditions in a CO_2 incubator (48, 49). The results suggest that synthesized Cs-Alg NPs can be used as vehicles for delivering probiotics. At higher concentrations, cationic polymers might interact with extracellular matrix components and alter cell membrane integrity, thereby hindering nanoparticle internalization.

3.5. MIC of amoxicillin for probiotics

The well-diffusion technique was employed to find the minimal inhibitory concentration of amoxicillin (Amx) against probiotics by determining the zone of inhibition. Five wells were created, and amoxicillin was added at increasing concentrations as 0, 10, 20, 40, and 50 µM (**Figure 3C**). After overnight incubation, the zones were measured at different angles, and their average was taken to find out the MIC. At 0 and 10 µM concentrations, there was no zone observed. The zone of inhibition started from a 20 µM concentration, and this was chosen as the MIC to inhibit the growth of probiotics.

Table 2. The CFU/mL was calculated to establish the effective role of Cs-Alg+ProB NPs in the presence of antibiotics

S. No.	Sample	Absorbance at 600 nm	CFU/mL
1.	Free Probiotic (FPB)	1.954	$2.0 \pm 0.07 \times 10^9$
2.	Free Probiotic + Amoxicillin (FPB+Amx)	0.270	$2.7 \pm 0.05 \times 10^8$
3.	Cs-Alg+ProB NPs (CPB)	1.883	$1.9 \pm 0.07 \times 10^9$
4.	Cs-Alg+ProB NPs + Amoxicillin (CPB+Amx)	1.413	$1.4 \pm 0.1 \times 10^9$

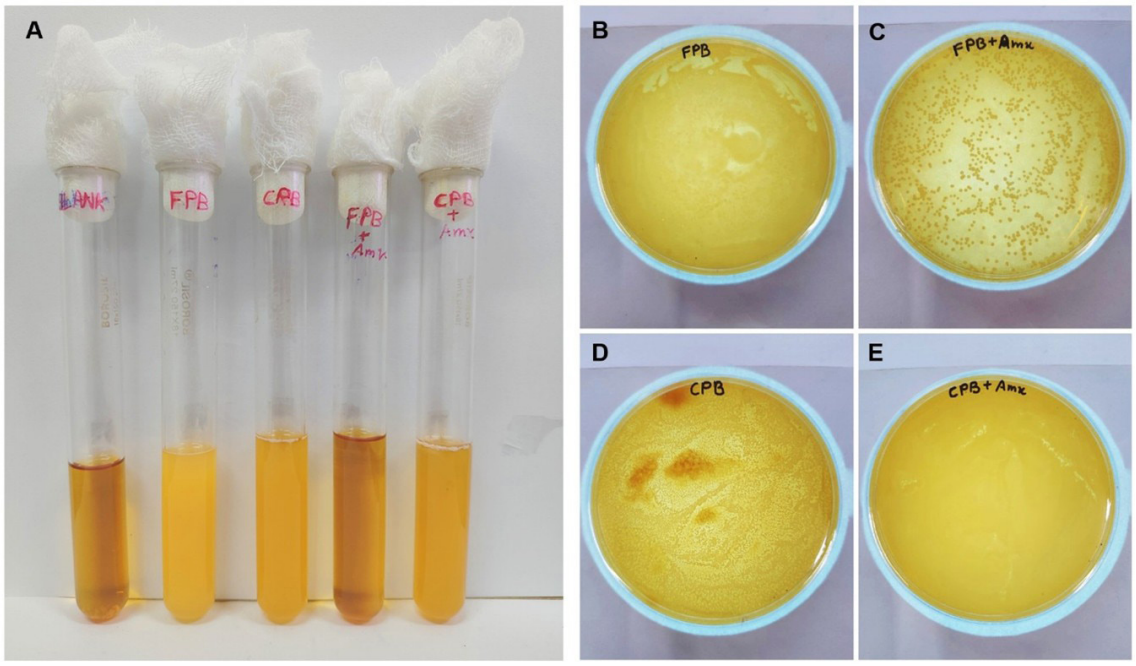

Figure 4. Cs-Alg NPs encapsulation protects probiotics against antibiotics (amoxicillin). **(A)** Coincubation of free probiotics & encapsulated probiotics with amoxicillin for 24 h. **(B)** 12 h incubation of free probiotics. **(C)** coincubation of free probiotics and amoxicillin. **(D)** 12 h incubation of Cs-Alg NPs loaded probiotics. **(E)** 12 h coincubated of Cs-Alg NPs loaded probiotics with amoxicillin ($p < 0.05$).

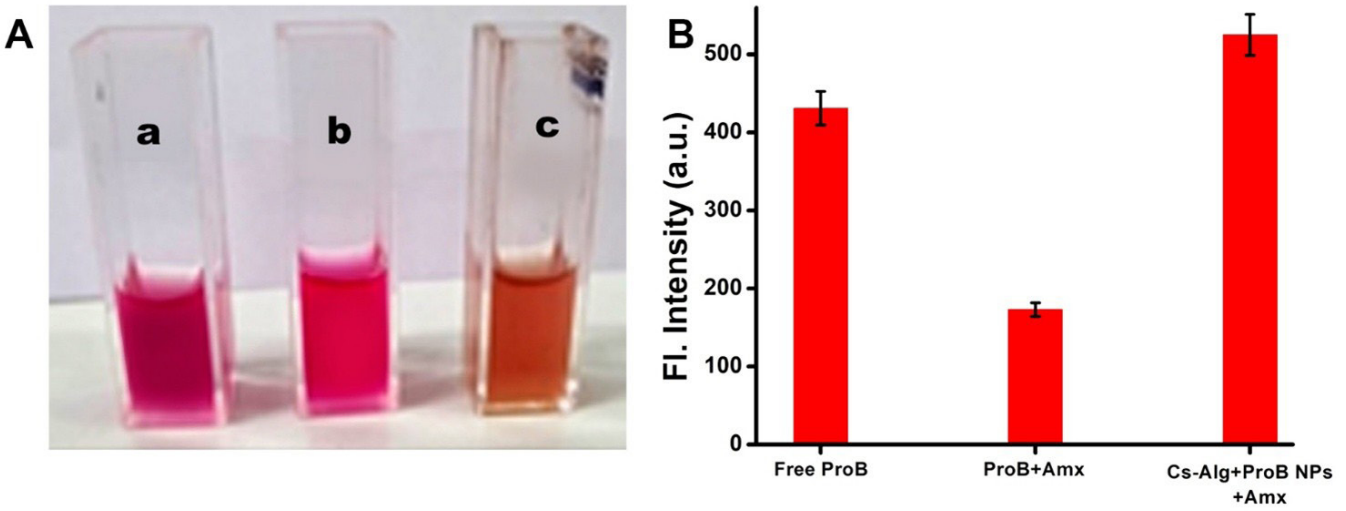

Figure 5. Effect of Cs-Alg NPs encapsulation on metabolic activity of probiotics after incubation in broth and amoxicillin, as quantified by Alamar Blue assay (a-Nanoformulated probiotics+drug, b-Free probiotics+drug, and c-probiotics). **(A)** 3h incubated tubes with Alamar blue dye. **(B)** Fluorescence intensity of the incubated samples.

3.6. Co-incubation of drugs and probiotics

To illustrate the benefits of co-administration of antibiotics alongside encapsulated probiotics, we assessed this combined treatment strategy. Injuries can create clinical challenges due to an enhanced inflammatory response caused by mixed infections, which hinders the typical healing process. While normal wound recovery typically takes two to four weeks, chronic wounds do not achieve skin integrity for over three months. The two antibiotic-resistant bacteria most commonly associated with chronic wounds are *Staphylococcus aureus* (SA) and *Pseudomonas aeruginosa* (PA). Both SA and PA are known to produce biofilms that reduce the effectiveness of antibiotics, disrupt wound healing, and are resistant to various antibiotic classes. We predicted that the co-incubation of antibiotics and probiotics would help to treat these infections. By releasing antimicrobial compounds, including organic acids, bacteriocins, and biosurfactants, probiotics generally help fight pathogenic bacteria. These substances not only stop harmful pathogens from adhering to bodily surfaces but also dissolve the protective biofilm these pathogens employ to guard themselves. Once the biofilm is weakened, antibiotics can more effectively kill the harmful bacteria. However, there is a significant downside: antibiotics do not distinguish between good and bad bacteria, so they often end up killing the beneficial probiotics as well. This can disrupt the balance of the gut microbiome and reduce the overall effectiveness of the treatment. That is why it is important to find ways to protect probiotics during antibiotic therapy so they can continue to support the body's defenses without being wiped out themselves.

As a proof of concept, free and encapsulated probiotics, with or without antibiotics, were introduced into the broth and incubated for 24 hours, as shown in **Figure 4A**. In the absence of amoxicillin, both free (FPB) and Cs-Alg+ProB NPs (CPB) show similar growth by measuring their absorbance at 600 nm (**Figure 4B and D**). From this, 100 µL was taken and inoculated in MRS agar, and the CFU/mL was counted as 2.0×10^9 and 1.9×10^9. These results suggest that encapsulation did not affect the growth of probiotics. In the presence of amoxicillin, free (FPB+Amx) and Cs-Alg+ProB NPs (CPB+Amx) were added to the medium and incubated. After incubation, the growth of probiotics in FPB+Amx was inhibited by antibiotics; however, in CPB+Amx, the growth was almost similar to that of FPB and CPB (**Table 2**). Then, the CFU/mL was found to be 2.7×10^8 for FPB+Amx (**Figure 4C**) and 1.4×10^9 for CPB+Amx (**Figure 4E**). These results show that the chitosan alginate NPs encapsulation method discussed above was effective in protecting probiotics from the antibiotic amoxicillin.

3.7. AlamarBlue assay for metabolic activity study

The Alamar blue assay is based on the reduction of resazurin, a non-fluorescent blue dye, into resorufin, a pink and highly fluorescent compound, by metabolically active cells. This reduction is a direct indicator of cellular respiration and metabolic activity. After incubation, the colour change was observed from blue to pink, and pale yellow reflects the viability and metabolic state of the probiotics (**Figure 5A**). This colour change is due to bacterial metabolic activity, which reduces resazurin to resorufin, a pink compound. The higher bacterial activity further reduced resorufin to hydroresorufin, which is colourless or pale yellow. The fluorescence was further quantified using a spectrofluorometer (excitation at 530 nm), where higher fluorescence intensity corresponded to greater bacterial metabolic activity (**Figure 5B**). The major advantage of the Alamar blue assay is that it is non-destructive, highly sensitive, and allows

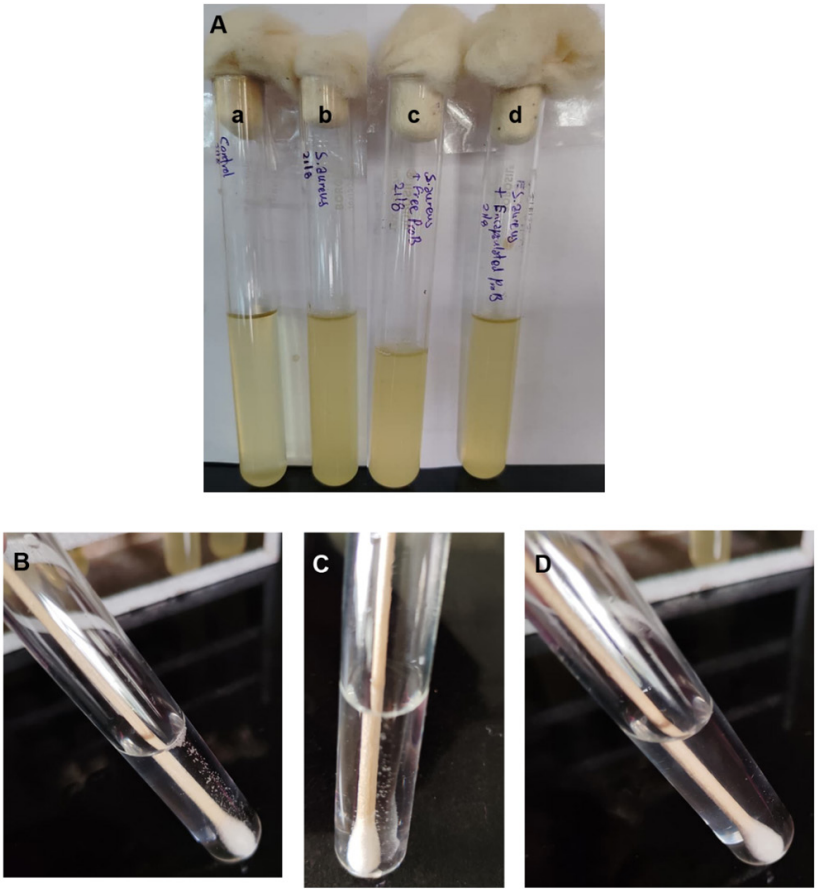

Figure 6: (A) Co-incubation of probiotics with *S. aureus* in the presence of amoxicillin (**a**-blank, **b**-*S. aureus* with Amx, **c**-*S. aureus* with free probiotics and Amx, and **d**-*S. aureus* with encapsulated probiotics and Amx). **(B)** Catalyse test of *S. aureus* incubated with amoxicillin. **(C)** Catalyse test of *S. aureus* incubated with free probiotics and amoxicillin. **(D)** Catalyse test of *S. aureus* incubated with Cs-Alg+ProB NPs and amoxicillin.

real-time monitoring of cell viability without harming the cells. Unlike other assays, such as MTT or trypan blue exclusion, Alamar blue does not require cell lysis or termination, making it particularly suitable for probiotics, where maintaining viability is critical. Additionally, it provides both qualitative (colorimetric) and quantitative (fluorometric) readouts, ensuring accuracy and reproducibility. The study shows that free probiotics growth was used as a control, compared with which, probiotics incubated with amoxicillin showed only 40% growth. The Cs-Alg+ProB NPs showed significantly higher metabolic activity compared to free probiotics under antibiotic stress, confirming that encapsulation offers protection and enhances viability.

3.8. Co-incubation of probiotics

To demonstrate the utility of the co-administration of amoxicillin with encapsulated probiotics, we evaluated this approach with bacteria that are relevant to chronic infections (**Figure 6A**). Chronic infections pose clinical complications because bacteria can evade host defences and persist for weeks or months. Such infections are often caused by *Mycobacterium tuberculosis*, *Helicobacter pylori*, *Staphylococcus aureus*, and *Pseudomonas aeruginosa*. Among these, *S. aureus* is considered particularly dangerous due to its unique virulence factors, survival strategies, and antibiotic resistance mechanisms. Methicillin-resistant *Staphylococcus aureus* (MRSA), a multi-resistant strain of *S. aureus*, represents a major therapeutic challenge. We therefore chose the culture of *S. aureus* as our model system.

The antibacterial efficiency of *S. aureus* was evaluated using the catalase assay. Typically, *S. aureus* is catalase-positive (vigorous bubbles), whereas most probiotic strains are catalase-negative (no bubbles). After 24 h incubation, *S. aureus* incubated with the antibiotic showed catalase positive (**Figure 6B**), indicating antibiotic resistance. When free probiotics were co-incubated with *S. aureus* in the presence of amoxicillin, they showed catalase-positive, suggesting that the antibiotics killed probiotics while *S. aureus* was alive (**Figure 6C**). In contrast, when encapsulated probiotics were co-incubated with *S. aureus* in the presence of antibiotics, catalase activity was negative (**Figure 6D**). This indicates that encapsulated probiotics have shown antimicrobial effects on S. aureus, attributed to the production of organic acids, bacteriocins, and biosurfactants. These findings demonstrate that encapsulation protects probiotics from amoxicillin and enhances their antibacterial efficacy, which is needed for successful eradication of pathogens.

4. Conclusion

In summary, the ionic gelation technique was utilized to synthesize probiotic-loaded chitosan-alginate nanoparticles (Cs-Alg+ProB NPs) to address the challenges associated with the combined administration of antibiotics and probiotics. The DLS analysis indicated that the hydrodynamic diameter and zeta potential of Cs-Alg NPs are 280±7.10 nm and -18.3 mV, and it became 328.7±13.07 nm and -22 mV for Cs-Alg+ProB NPs. This increase in size and alteration in surface charge suggest changes in the microenvironment, confirming the successful encapsulation of probiotics within Cs-Alg NPs. Release kinetics revealed an initial burst release and then a sustained release for 600 minutes, while a higher rate of release was found in an acidic compared to a neutral environment. Based on the Korsmeyer-Peppas model, the release process of prepared Cs-Alg NPs was Fickian diffusion. In addition, the NPs demonstrated better swelling properties in an acidic medium compared to a neutral one. The safety of the delivery system, Cs-Alg NPs, was confirmed by performing the cell viability assays (bovine fibroblasts). But the difficulty for this work is that it was difficult to search for a CFU of S. aureus specific strain when co-incubating with probiotics together. To overcome this issue, we performed a catalase test because probiotics are catalase-negative and *S. aureus* is catalase-positive. Coincubation experiments demonstrated that the nanoparticles effectively shield probiotics from the antibacterial effects of antibiotics. Consequently, the mixed polymer nanoparticles improve solubility, biocompatibility, pH-responsive release, and protect probiotics from antibiotics/harsh environments, presenting a promising alternative for addressing multidrug resistance and enhancing therapeutic efficacy.

When taken orally, probiotics are susceptible to oxygen, bile, and stomach acid, as well as antibiotic therapy used in conjunction with the administration of the probiotics. Although classic tools, as nutrient and Streptococcus thermophilus resistant strain selection, are useful, micro- and nano-encapsulation nowadays is the most efficient technology. Introducing a process to increase the stability, survival , and targeted delivery of probiotics through protective encapsulation. It enriches their bioavailability and product value. But there are serious and valid safety issues with nanotechnology. Size, presence of surface-bound moieties, and dosage are among the variables that influence the behavior of nanomaterials. Once inside the body, they can pass through fragile barriers or have adverse effects on cells, which can result in inflammation, oxidative stress, and protein or nucleic acid injury. Similarly, selecting suitable materials for nanoencapsulation formulation is another significant challenge. Every nano-based system must therefore be designed using biocompatible materials and thoroughly tested in both laboratory and animal experiments. Although regulatory frameworks exist, such as those of the FDA and the European Commission, more stringent guidelines are needed to ensure the safety, efficacy, and environmental responsibility of nanomaterials used in probiotic formulations.

Acknowledgment

CARE is acknowledged for providing infrastructure. AT acknowledges CARE for the research fellowship and other facilities.

Competing interest

The authors have no relevant financial or non-financial interest to declare.

Data availability statement

The data supporting this article have been included in the manuscript.

Funding

The authors declare that no funds or grants were received during the preparation of this article.

Ethics approval

Not applicable

Authors contribution

Anbazhagan Thirumalai: Conceptualization, Methodology, Formal analysis and investigation, Writing-original draft preparation. Sampreeti Chatterjee & Pemula Gowtham: Methodology, Formal analysis, validation. Koyeli Girigoswami: Formal analysis, Validation, Writing-review, and editing. Agnishwar Girigoswami: Conceptualization, Methodology, Formal analysis, Supervision, Project administration, Writing- Review and Editing.

References

1. Elshobary ME, Badawy NK, Ashraf Y, Zatioun AA, Masriya HH, Ammar MM, et al. Combating Antibiotic Resistance: Mechanisms, Multidrug-Resistant Pathogens, and Novel Therapeutic Approaches: An Updated Review. Pharmaceuticals. 2025;18(3):402.
2. Anupama A, Pattapulavar V, Christopher JG. The past, present, future of Listeria monocytogenes: Understanding the molecular pathways, antibiotic resistance and public health implications. Medicine in Microecology. 2025;25:100127.
3. Naseef Pathoor N, Vijetha V, Sankar GP, and Gopal RK. From resistance to treatment: the ongoing struggle with Acinetobacter baumannii. Critical Reviews in Microbiology. 2025:1–22.
4. Boopathi TS, Rajiv A, Patel TSGM, Bareja L, Salmen SH, Aljawdah HM, et al. Efficient one-pot green synthesis of carboxymethyl cellulose/folic acid embedded ultrafine CeO2 nanocomposite and its superior multi-drug resistant

antibacterial activity and anticancer activity. Bioprocess and Biosystems Engineering. 2025;48(1):121–31.
5. Fanelli U, Chiné V, Pappalardo M, Gismondi P, Esposito S. Improving the quality of hospital antibiotic use: Impact on multidrug-resistant bacterial infections in children. Frontiers in pharmacology. 2020;11:745.
6. Naseef Pathoor N, Viswanathan A, Wadhwa G, Ganesh PS. Understanding the biofilm development of Acinetobacter baumannii and novel strategies to combat infection. APMIS. 2024;132(5):317–35.
7. Cotugno S, De Vita E, Frallonardo L, Novara R, Papagni R, Asaduzzaman M, et al. Antimicrobial Resistance and Migration: Interrelation Between Two Hot Topics in Global Health. Ann Glob Health. 2025;91(1):12.
8. Tahmasebi H, Arjmand N, Monemi M, Babaeizad A, Alibabaei F, Alibabaei N, et al. From Cure to Crisis: Understanding the Evolution of Antibiotic-Resistant Bacteria in Human Microbiota. Biomolecules. 2025;15(1):93.
9. Dai C, Liu Y, Lv F, Cheng P, Qu S. An alternative approach to combat multidrug-resistant bacteria: new insights into traditional Chinese medicine monomers combined with antibiotics. Advanced Biotechnology. 2025;3(1):6.
10. Kumar S, Mahato RP, Ch S, Kumbham S. Current strategies against multidrug-resistant Staphylococcus aureus and advances toward future therapy. The Microbe. 2025;6:100281.
11. Cox D. Antibiotic resistance: the race to stop the silent tsunami facing modern medicine. The Guardian. 2015;41(5):320–7.
12. Wilson BA, Garud NR, Feder AF, Assaf ZJ, Pennings PS. The population genetics of drug resistance evolution in natural populations of viral, bacterial and eukaryotic pathogens. Molecular Ecology. 2016;25(1):42–66.
13. Exner M, Bhattacharya S, Christiansen B, Gebel J, Goroncy-Bermes P, Hartemann P, et al. Antibiotic resistance: What is so special about multidrug-resistant Gram-negative bacteria? GMS Hyg Infect Control. 2017;12:Doc05.
14. Ruppé É, Woerther P-L, Barbier F. Mechanisms of antimicrobial resistance in Gram-negative bacilli. Annals of Intensive Care. 2015;5(1):21.
15. Scoffone VC, Trespidi G, Barbieri G, Arshad A, Israyilova A, Buroni S. The Evolution of Antimicrobial Resistance in Acinetobacter baumannii and New Strategies to Fight It. Antibiotics. 2025;14(1):85.
16. La Rosa MC, Maugeri A, Favara G, La Mastra C, Magnano San Lio R, Barchitta M, et al. The Impact of Wastewater on Antimicrobial Resistance: A Scoping Review of Transmission Pathways and Contributing Factors. Antibiotics. 2025;14(2):131.
17. Partridge SR. Analysis of antibiotic resistance regions in Gram-negative bacteria. FEMS microbiology reviews. 2011;35(5):820–55.
18. Kadri SS. Key Takeaways From the U.S. CDC's 2019 Antibiotic Resistance Threats Report for Frontline Providers. Critical Care Medicine. 2020;48(7):939–45.
19. Wang H, Thomas PPM. The Burden of Antimicrobial Resistant Infections in Wales: a population-level modelling analysis. European Journal of Public Health. 2020;30(Supplement_5):ckaa166.702.
20. Alhassan MY, Ahmad AA. Antimicrobial resistance in a changing climate: a One Health approach for adaptation and mitigation. Bulletin of the National Research Centre. 2025;49(1):26.
21. Thakur R, Singh A, Dhanwar R, Kadam S, Waghmare U, Lodha T, et al. Global perspectives on residual antibiotics: environmental challenges and trends. Discover Sustainability. 2025;6(1):232.
22. Vuotto C, Longo F, Donelli G. Probiotics to counteract biofilm-associated infections: promising and conflicting data. International journal of oral science. 2014;6(4):189–94.
23. Gareau MG, Sherman PM, Walker WA. Probiotics and the gut microbiota in intestinal health and disease. Nature reviews Gastroenterology & hepatology. 2010;7(9):503–14.
24. Ng S, Hart A, Kamm M, Stagg A, Knight SC. Mechanisms of action of probiotics: recent advances. Inflammatory bowel diseases. 2009;15(2):300–10.
25. Ouwehand AC, Sofia F, A. HA, Anna L, and Stahl B. Probiotic approach to prevent antibiotic resistance. Annals of Medicine. 2016;48(4):246–55.
26. Levy SB, Marshall B. Antibacterial resistance worldwide: causes, challenges and responses. Nature medicine. 2004;10(Suppl 12):S122–S9.
27. Snydman DR. The safety of probiotics. Clinical infectious diseases. 2008;46(Supplement_2):S104–S11.
28. Thirumalai A, Girigoswami K, Harini K, Pallavi P, Gowtham P, Girigoswami A. A review of the current state of probiotic nanoencapsulation and its future prospects in biomedical applications. Biocatalysis and Agricultural Biotechnology. 2024;57:103101.
29. Thirumalai A, Elboughdiri N, Harini K, Girigoswami K, Girigoswami A. Phosphorus-carrying cascade molecules: inner architecture to biomedical applications. Turkish Journal of Chemistry. 2023;47(4):667–88.
30. Vega-Carranza AS, Cervantes-Chávez JA, Luna-Bárcenas G, Luna-González A, Diarte-Plata G, Nava-Mendoza R, et al. Alginate microcapsules as delivery and protective systems of Bacillus licheniformis in a simulated shrimp's digestive tract. Aquaculture. 2021;540:736675.
31. Yuan L, Wei H, Yang X-Y, Geng W, Peterson BW, van der Mei HC, et al. Escherichia coli Colonization of Intestinal Epithelial Layers In Vitro in the Presence of Encapsulated Bifidobacterium breve for Its Protection against Gastrointestinal Fluids and Antibiotics. ACS Applied Materials & Interfaces. 2021;13(14):15973–82.
32. Li Z, Behrens AM, Ginat N, Tzeng SY, Lu X, Sivan S, et al. Biofilm- inspired encapsulation of probiotics for the treatment of complex infections. Advanced Materials. 2018;30(51):1803925.

33. Pallavi P, Girigoswami K, Harini K, Gowtham P, Thirumalai A, Girigoswami A. Theranostic dye entrapped in an optimized blended-polymer matrix for effective photodynamic inactivation of diseased cells. Naunyn-Schmiedeberg's Arch Pharmacol. 2025;398(1):867–80.
34. Gazori T, Khoshayand MR, Azizi E, Yazdizade P, Nomani A, Haririan I. Evaluation of alginate/chitosan nanoparticles as antisense delivery vector: formulation, optimization and in vitro characterization. Carbohydrate Polymers. 2009;77(3):599–606.
35. Thirumalai A, Harini K, Pallavi P, Gowtham P, Girigoswami K, Girigoswami A. Bile salt-mediated surface-engineered bilosome-nanocarriers for delivering therapeutics. Nanomedicine Journal. 2024;11(1):1–12.
36. Girigoswami K, Girigoswami A. Encapsulation of Beta-lactam Antibiotic Amoxicillin in Chitosan-alginate Nanohydrogels to Improve Antibacterial Efficacy. Nanomedicine Research Journal. 2023;8(4):335–44.
37. Bhoopathy J, Weslen VS, Vedha YB, Selvarajan R, Sankari D, Jayashri S, et al. Haemostatic potency of sodium alginate/aloe vera/sericin composite scaffolds – preparation, characterisation, and evaluation. Artificial Cells, Nanomedicine, and Biotechnology. 2024;52(1):35–45.
38. Harini K, Girigoswami K, Thirumalai A, Girigoswami A. Polymer-Based Antimicrobial Peptide Mimetics for Treating Multi-drug Resistant Infections: Therapy and Toxicity Evaluation. International Journal of Peptide Research and Therapeutics. 2024;30(6):64.
39. Manivannan S, Narayan S. Studies on polyethylene glycol crosslinked chitosan nanoparticles for co-delivery of docetaxel and 5-fluorouracil with synergistic effect against cancer. Macromolecular Research. 2024;32(4):371–92.
40. Divya K, Jisha MS. Chitosan nanoparticles preparation and applications. Environmental Chemistry Letters. 2018;16(1):101–12.
41. A H, Sofini SPS, Balasubramanian D, Girigoswami A, Girigoswami K. Biomedical applications of natural and synthetic polymer based nanocomposites. Journal of biomaterials science Polymer edition. 2024;35(2):269–94.
42. Thirumalai A, Girigoswami K, Harini K, Kiran V, Durgadevi P, Girigoswami A. Natural polymer derivative-based pH-responsive nanoformulations with entrapped diketo-tautomers of 5-fluorouracil for enhanced cancer therapy: Original scientific article. ADMET and DMPK. 2025;13(1):2554.
43. Ge M, Li Y, Zhu C, Liang G, S.M JA, Hu G, et al. Preparation of organic-modified magadiite–magnetic nanocomposite particles as an effective nanohybrid drug carrier material for cancer treatment and its properties of sustained release mechanism by Korsmeyer–Peppas kinetic model. Journal of Materials Science. 2021;56(25):14270–86.
44. Thirumalai A, Girigoswami K, Prabhu AD, Durgadevi P, Kiran V, Girigoswami A. 8-Anilino-1-naphthalenesulfonate-Conjugated Carbon-Coated Ferrite Nanodots for Fluoromagnetic Imaging, Smart Drug Delivery, and Biomolecular Sensing. Pharmaceutics. 2024;16(11):1378.
45. Jaiganesh T, Daisy Vimala Rani J, Girigoswami A. Spectroscopically characterized cadmium sulfide quantum dots lengthening the lag phase of Escherichia coli growth. Spectrochimica Acta Part A: Molecular and Biomolecular Spectroscopy. 2012;92:29–32.
46. Gómez Chabala LF, Cuartas CE, López ME. Release Behavior and Antibacterial Activity of Chitosan/Alginate Blends with Aloe vera and Silver Nanoparticles. Mar Drugs [Internet]. 2017; 15(10):[328 p.].
47. Mercy DJ, Harini K, Madhumitha S, Anitha C, Iswariya J, Girigoswami K, et al. pH-responsive polymeric nanostructures for cancer theranostics. Journal of Metals, Materials and Minerals. 2023;33(2):1–15.
48. van Stevendaal MHME, Vasiukas L, Yewdall NA, Mason AF, van Hest JCM. Engineering of Biocompatible Coacervate-Based Synthetic Cells. ACS Applied Materials & Interfaces. 2021;13(7):7879–89.
49. Kim T, Momin E, Choi J, Yuan K, Zaidi H, Kim J, et al. Mesoporous Silica-Coated Hollow Manganese Oxide Nanoparticles as Positive T1 Contrast Agents for Labeling and MRI Tracking of Adipose-Derived Mesenchymal Stem Cells. Journal of the American Chemical Society. 2011;133(9):2955–61.